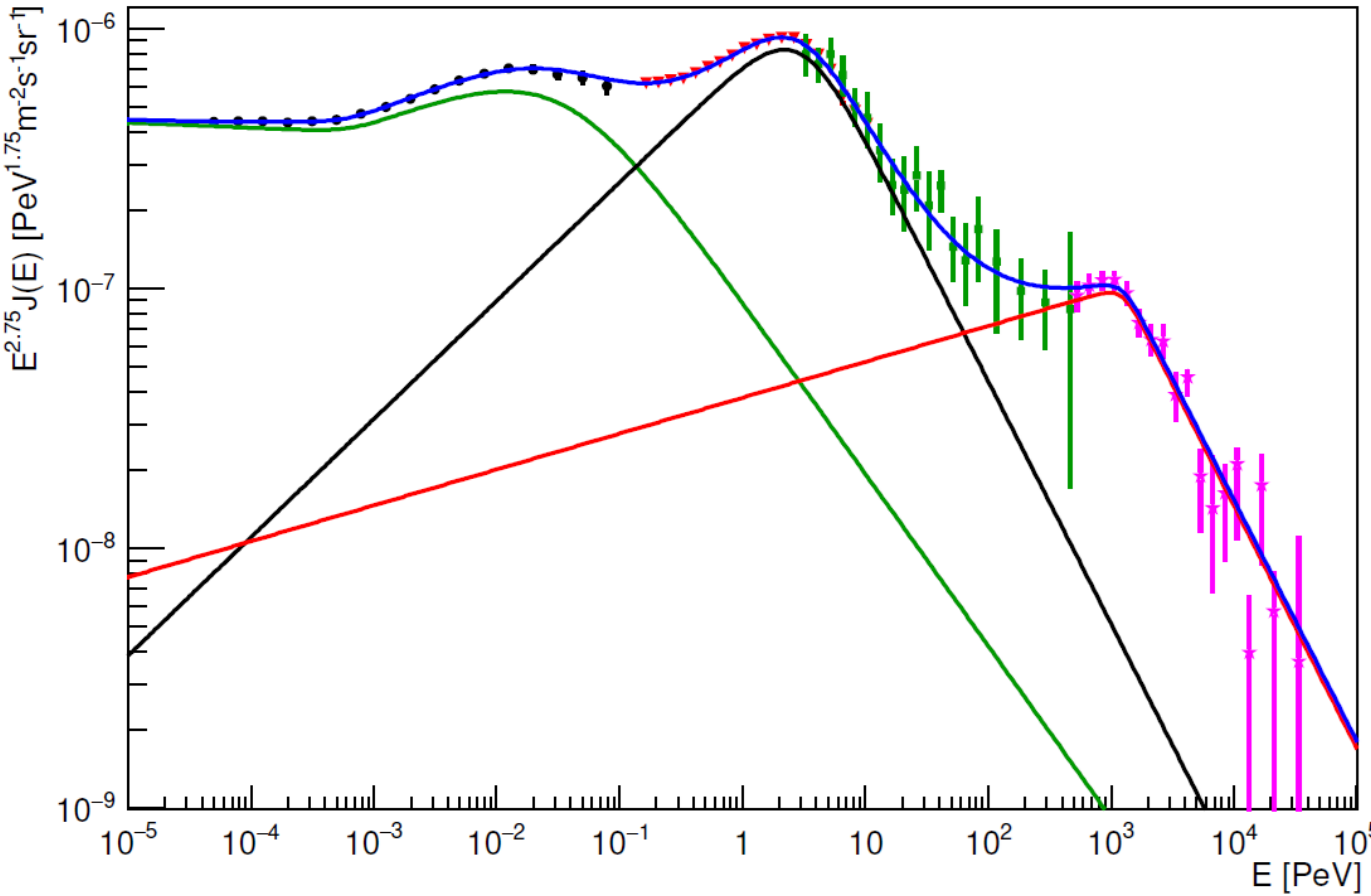
Cosmic rays from 1 GeV to 100 EeV due to star formation processes?



Some phenomenological fits at 40 GeV --- 500 PeV:
astro-ph/2606.02748v2 (2026) (submitted to MNRAS)

γ-ray signature of ultra high energy cosmic ray acceleration in GRB 221009A:
astro-ph/2604.10378 (2026), Section III

Issues at E > 500 PeV: paper in preparation

Timur DZHATDOEV (INR RAS), Anatoly SEMENOV (INR RAS / Lomonosov Moscow State University)

Proton spectrum of a single CR source

$$\frac{dN}{d\varepsilon} = K\varepsilon^{-\gamma} exp(-\varepsilon/\varepsilon_c)$$ power law with exponential cutoff (EPWL) spectrum

double log-parabola with exponential cutoff (EDLP) spectrum:

$$\frac{dN}{d\varepsilon} = K\varepsilon^{-\gamma+b\cdot ln(\varepsilon/\varepsilon_r) ln(\varepsilon/\varepsilon_c)} exp(-\varepsilon/\varepsilon_c)$$

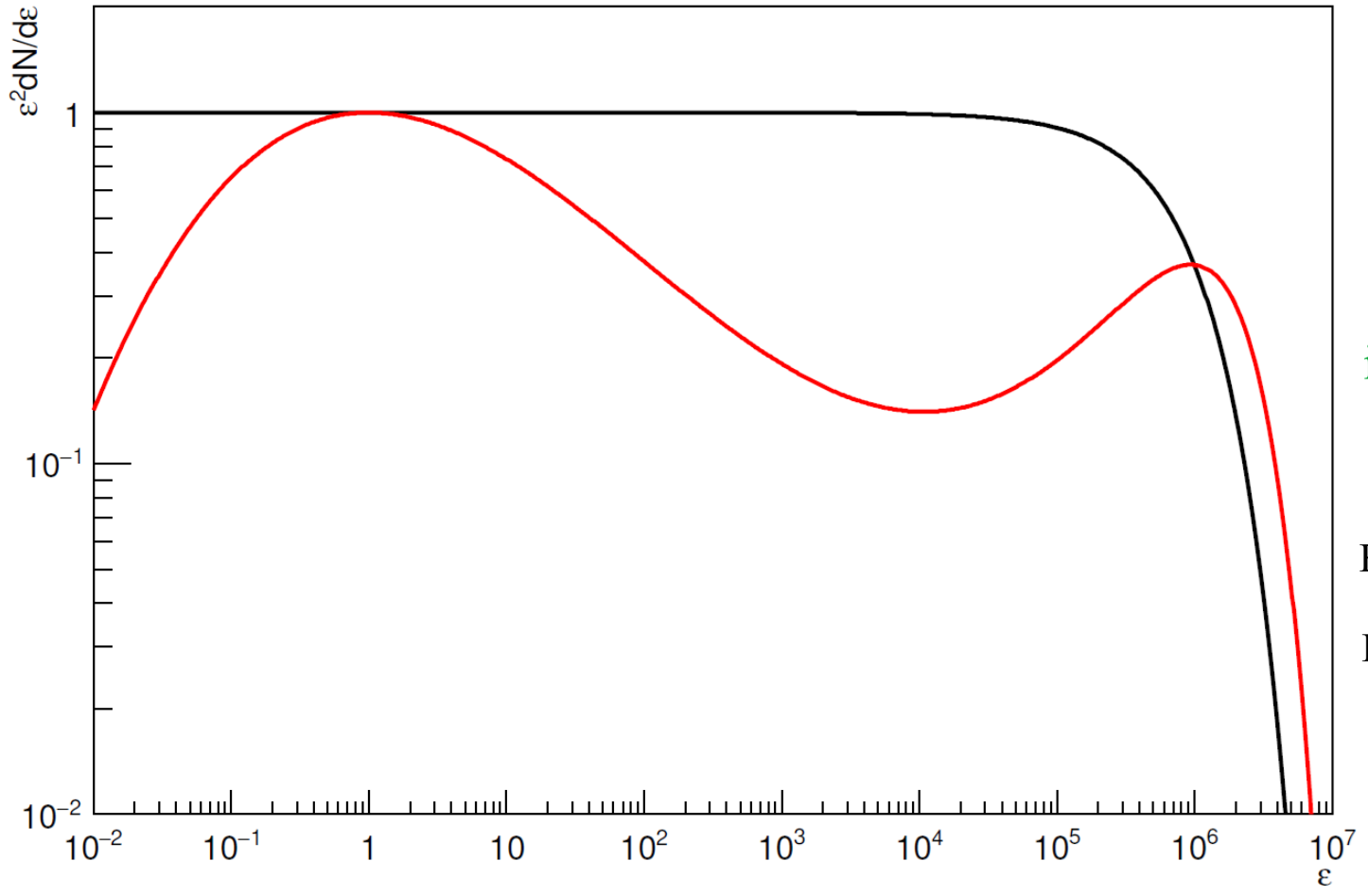
Proton spectrum for a population of CR sources

$$Q(E) = \int_{L_{min}}^{L_{max}} p(L) Q_s(E) dL$$

$$J(E) = K \left(\frac{E}{E_0}\right)^{-\gamma_1} \left[1 + \left(\frac{E}{E_a}\right)^{w_a}\right]^{-(\gamma_2-\gamma_1)/w_a} \times \left[1 + \left(\frac{E}{E_k}\right)^{w_k}\right]^{-(\gamma_3-\gamma_2)/w_k}$$

The observable intensity: the "smoothly broken power law with ankle" (SBPL-A) functional form

The proton spectrum of a single CR source: power law with exp. cutoff (EPWL, black) and double log-parabola with exp. cutoff (EDLP, red) spectra



$\varepsilon = E/m$

dimensionless kinetic energy

The convex shape is routinely reproduced in theoretical studies of particle acceleration in supernova remnants (SNRs)

Berezhko et al., JETP, **82**, 1 (1996)
Voelk et al., A&A, **396**, 649 (2002)
Berezhko et al., A&A, **400**, 971 (2003)
Ptuskin et al., ApJ, **718**, 31 (2010)
Ptuskin et al., Proc. 32nd ICRC (2011)

See also e.g. discussion in Hillas (2005)

Proton spectrum of a single CR source

$$\frac{dN}{d\varepsilon} = K\varepsilon^{-\gamma} exp(-\varepsilon/\varepsilon_c)$$ power law with exponential cutoff (EPWL) spectrum

double log-parabola with exponential cutoff (EDLP) spectrum:

$$\frac{dN}{d\varepsilon} = K\varepsilon^{-\gamma+b\cdot ln(\varepsilon/\varepsilon_r) ln(\varepsilon/\varepsilon_c)} exp(-\varepsilon/\varepsilon_c)$$

Proton spectrum for a population of CR sources

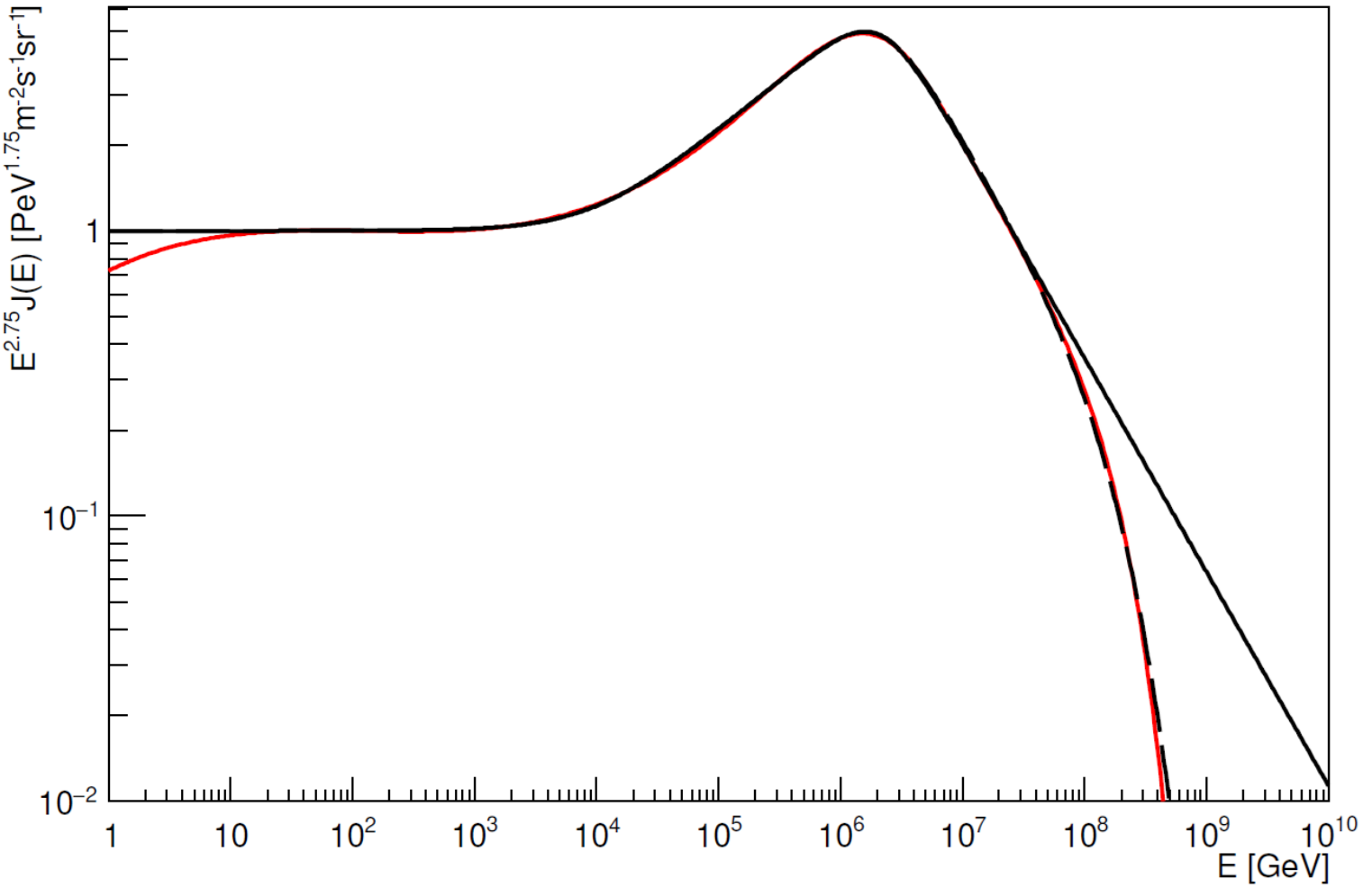
$$Q(E) = \int_{L_{min}}^{L_{max}} p(L) Q_s(E) dL$$

$$J(E) = K \left(\frac{E}{E_0}\right)^{-\gamma_1} \left[1 + \left(\frac{E}{E_a}\right)^{w_a}\right]^{-(\gamma_2-\gamma_1)/w_a} \times \left[1 + \left(\frac{E}{E_k}\right)^{w_k}\right]^{-(\gamma_3-\gamma_2)/w_k}$$

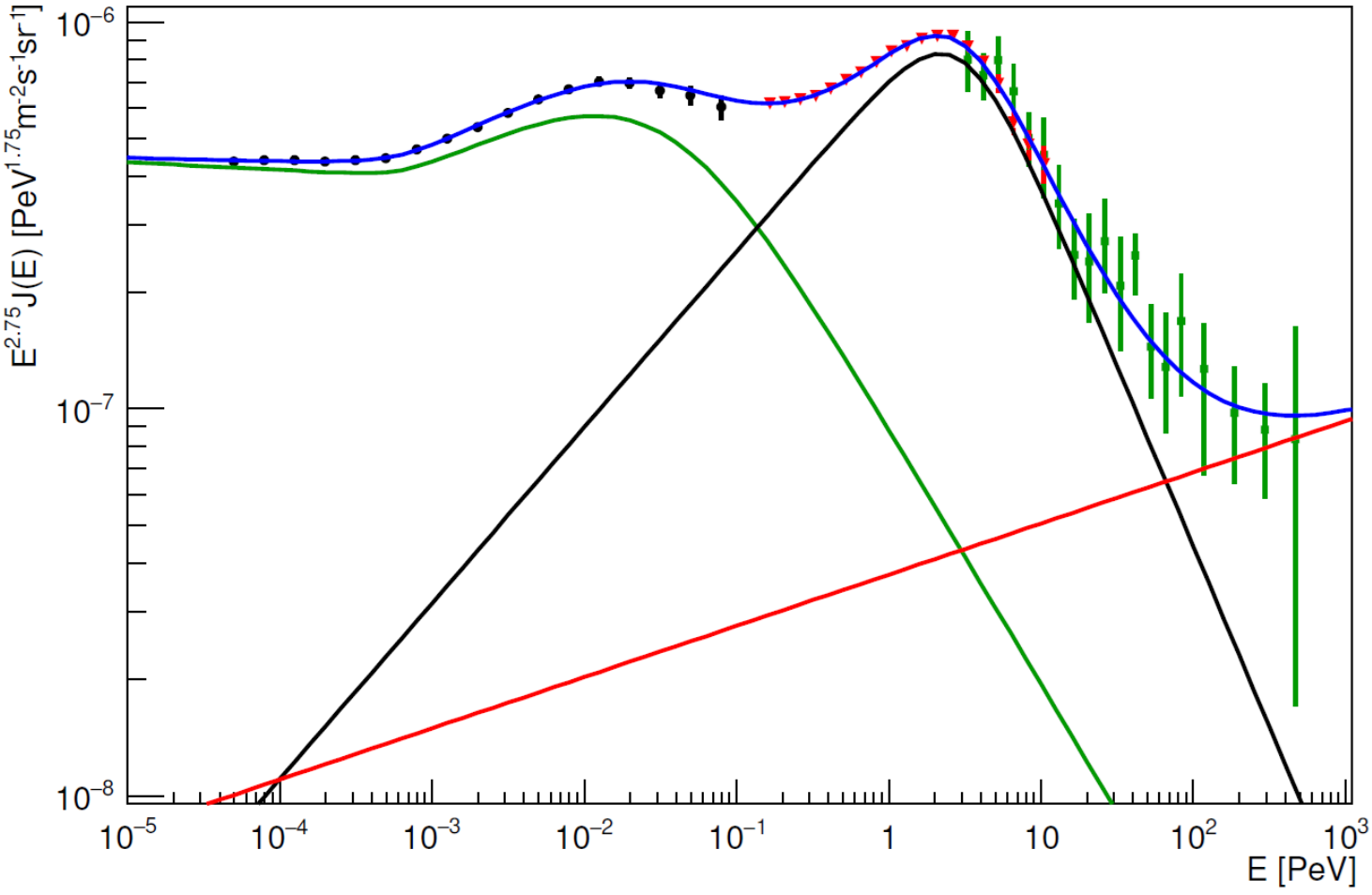
The observable intensity: the "smoothly broken power law with ankle" (SBPL-A) functional form

Proton spectrum for a population of CR sources

is well approximated with the SBPL-A functional form (black solid curve)



The proton CR spectrum



DAMPE (black circles)
An et al. (2019)
LHAASO (Cao et al., 2025)
IceTop (Aartsen et al., 2019, A19)

$K_E = 0.93$ for LHAASO and IceTop

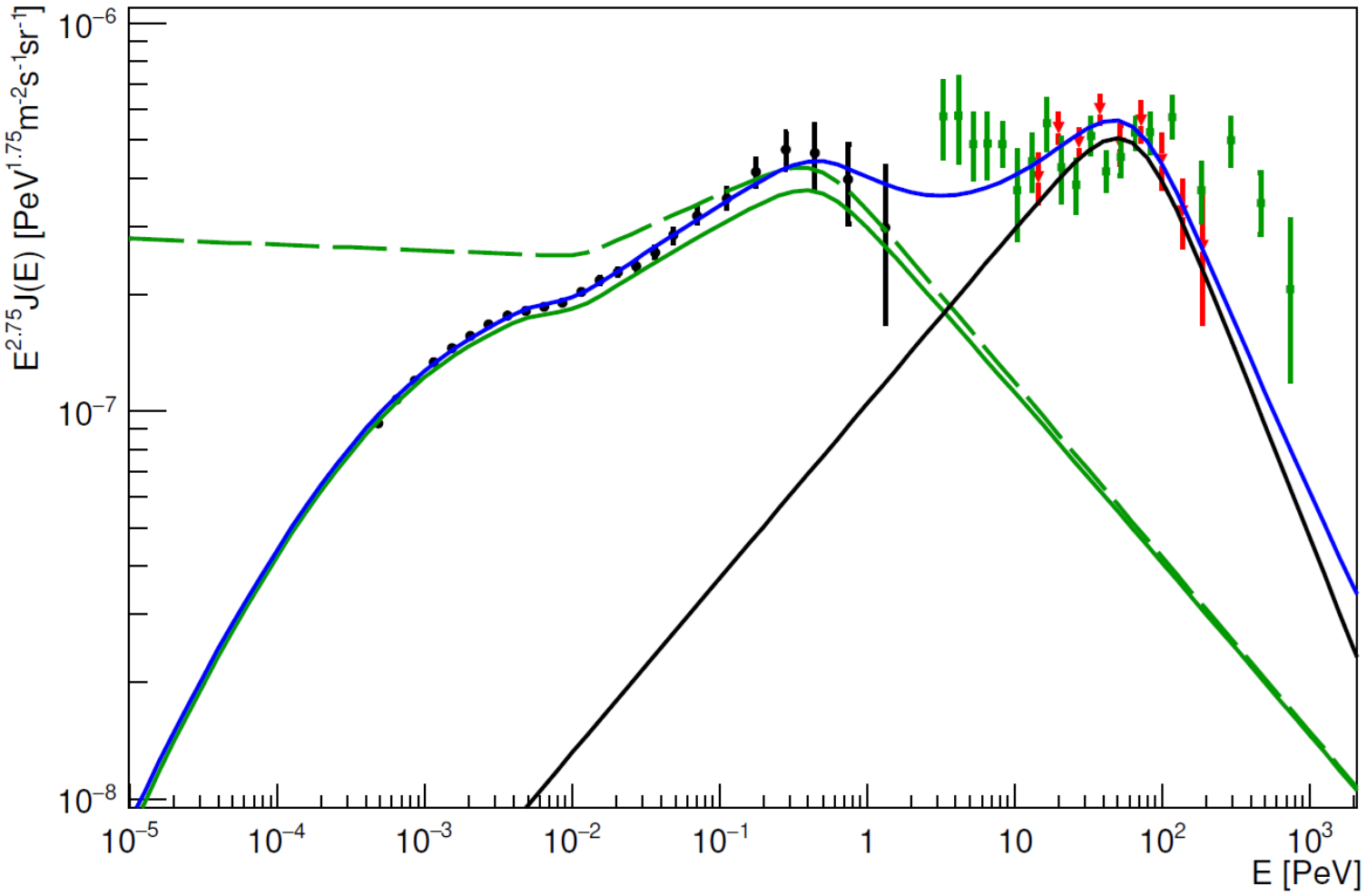
Star formation → SNRs → CR particle acceleration

Interpretation: two Galactic components (probably from SNRs) + one extragalactic component

Best-fit parameter values for the proton CR spectrum

parameter	value (MIGRAD)	value (MCMC)	uncertainties (MCMC)
K_1 [$\mathrm{PeV^{-1}m^{-2}s^{-1}sr^{-1}}$]	2.05×10^{-4}	2.14×10^{-4}	$+1.8\times10^{-5}$ -2.3×10^{-5}
γ_{11}	2.769	2.761	$+1.4\times10^{-2}$ -9.6×10^{-3}
γ_{12}	2.571	2.590	$+9.6\times10^{-3}$ -1.4×10^{-2}
γ_{13}	3.413	3.270	$+1.7\times10^{-1}$ -1.6×10^{-1}
E_a [PeV]	6.29×10^{-4}	6.27×10^{-4}	$+3.3\times10^{-5}$ -3.8×10^{-5}
E_{k1} [PeV]	3.50×10^{-2}	2.69×10^{-2}	$+8.2\times10^{-3}$ -6.4×10^{-3}
w_a	3.52	8.12	+18.9 -4.4
w_{k1}	1.20	1.59	+0.41 -0.30
K_2 [$\mathrm{PeV^{-1}m^{-2}s^{-1}sr^{-1}}$]	1.44×10^{-4}	1.34×10^{-4}	$+2.8\times10^{-5}$ -2.7×10^{-5}
γ_{21}	2.30	2.28	$+6.6\times10^{-2}$ -6.1×10^{-2}
γ_{22}	3.68	3.70	+0.17 -0.15
E_{k2} [PeV]	2.93	2.90	+0.34 -0.25
w_{k2}	2.44	2.65	+0.44 -0.34
K_3 [$\mathrm{PeV^{-1}m^{-2}s^{-1}sr^{-1}}$]	1.54×10^{-5}	1.58×10^{-5}	$+9.4\times10^{-6}$ -7.6×10^{-6}
γ_3	2.62	2.65	$+4.9\times10^{-2}$ -7.3×10^{-2}

The Iron spectrum: DAMPE (Alemanno et al., 2026 (A26), black circles);
KASCADE-Grande (Apel et al., 2013), IceTop

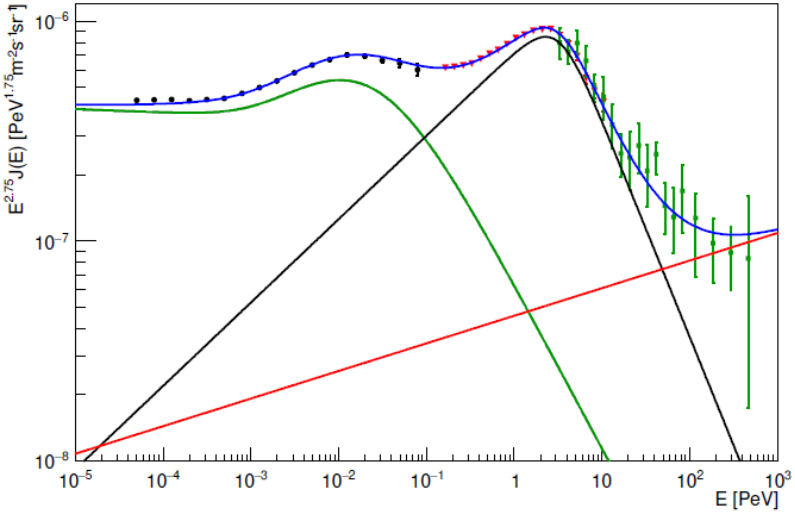


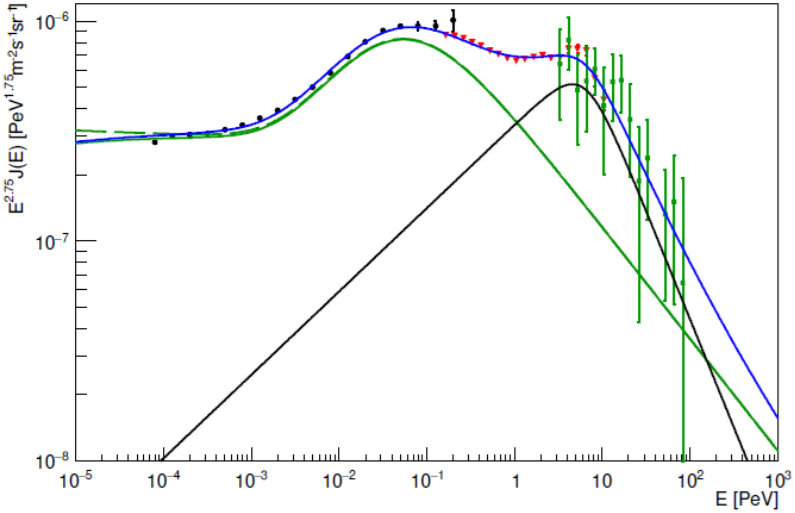
The effect of spallation is clearly visible: the difference between the solid and dashed green curves

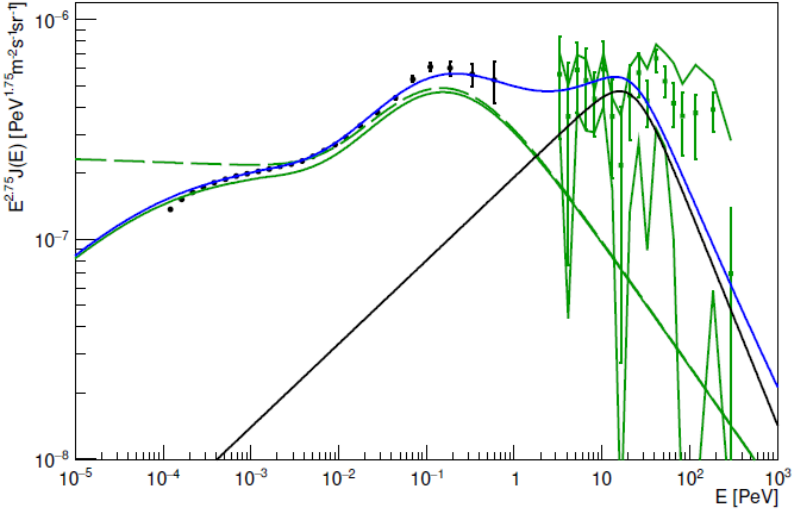
Best-fit parameter values for nuclei

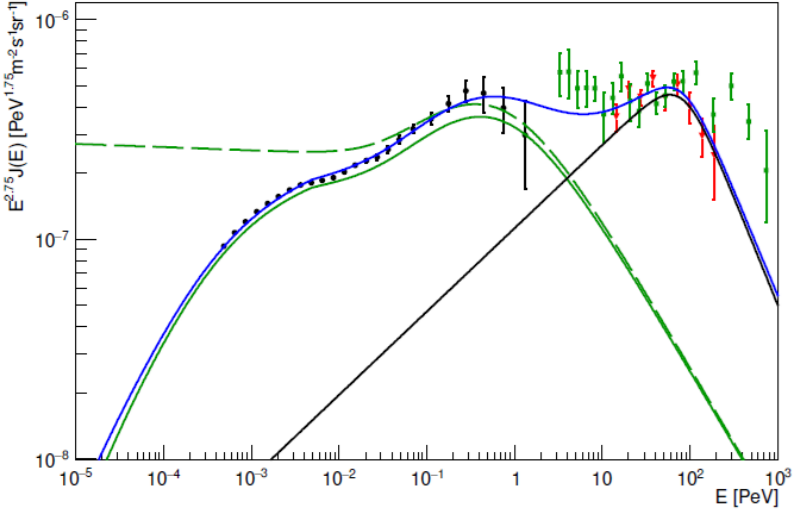
parameter	Helium (fit 1)	Helium (fit 2)	CNO	Iron
K_1 [$\mathrm{PeV^{-1}m^{-2}s^{-1}sr^{-1}}$]	1.54×10^{-4}	1.47×10^{-4}	1.20×10^{-4}	1.36×10^{-4}
γ_{11}	2.759	2.766	2.754	2.765
γ_{12}	2.355	2.353	2.400	2.580
γ_{13}	2.760	3.300	3.205	3.200
E_a [PeV]	1.50×10^{-3}	1.50×10^{-3}	7.00×10^{-3}	1.14×10^{-2}
E_{k1} [PeV]	3.45×10^{-2}	8.24×10^{-2}	0.146	0.468
w_a	1.07	1.22	1.94	9.76
w_{k1}	4.73	1.46	4.00	3.50
K_2 [$\mathrm{PeV^{-1}m^{-2}s^{-1}sr^{-1}}$]	4.34×10^{-5}	7.30×10^{-4}	4.35×10^{-5}	2.09×10^{-5}
γ_{21}	1.91	2.30	2.40	2.30
γ_{22}	4.18	3.73	3.24	3.71
E_{k2} [PeV]	5.92	6.06	30.0	62.9
w_{k2}	1.26	3.54	3.00	3.11

Proton (top-left), Helium (top-right), CNO (bottom-left), and Iron spectra









The datasets:

Helium: A26, LHAASO (Cao et al., 2026), Ice-Top (A19)

CNO: A26, Ice-Top (A19)

The effect of spallation is significant for the CNO and modest for the Helium spectrum

Best-fit parameter values for proton, Helium, CNO, and Iron spectra

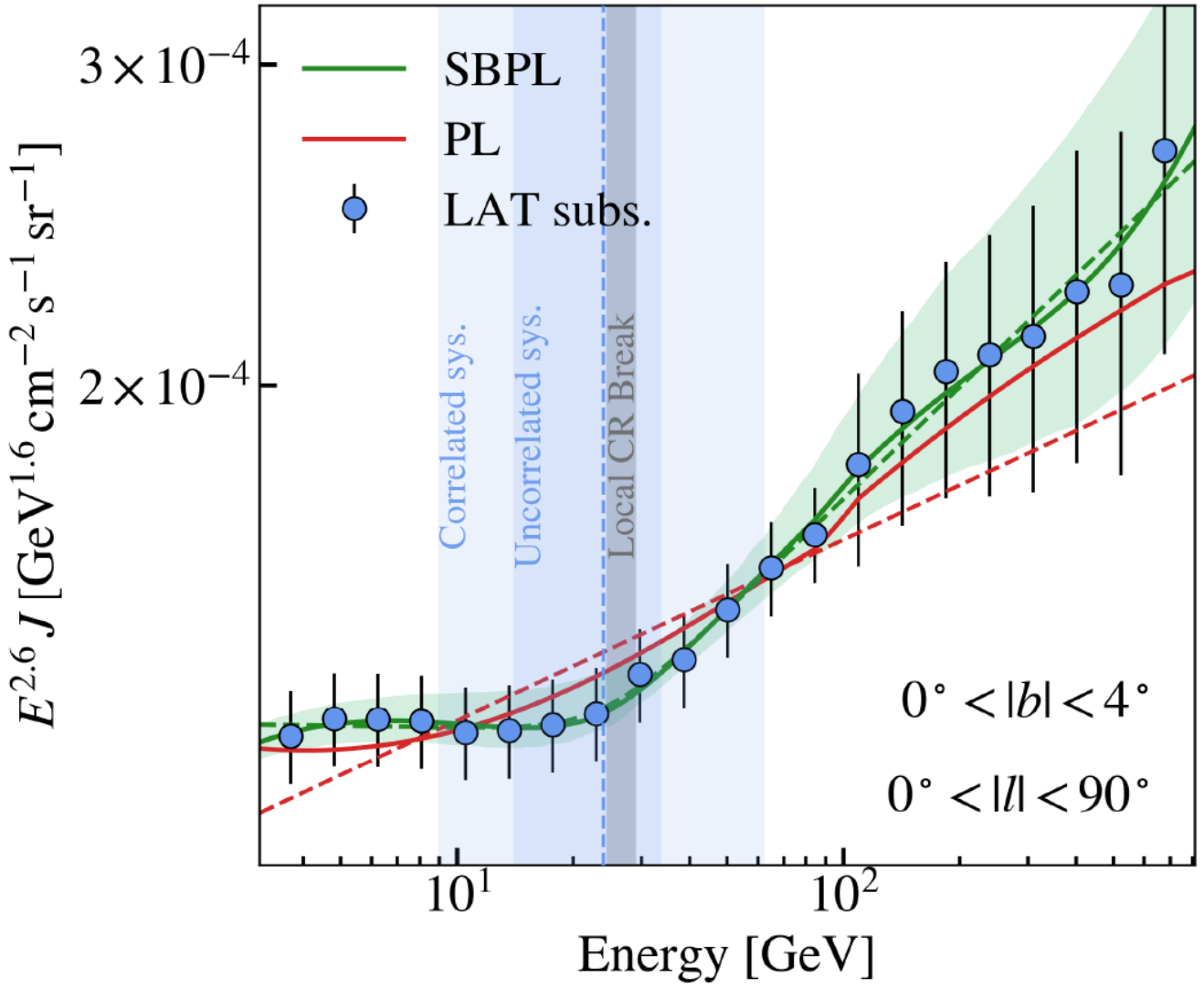
parameter	value (MIGRAD)	value (MCMC)	uncertainties (MCMC)
K_{1-p} [PeV^{-1}m^{-2}s^{-1}sr^{-1}]	1.96×10^{-4}	1.81×10^{-4}	$+9.6\times10^{-6}$ -9.4×10^{-6}
K_{1-h} [PeV^{-1}m^{-2}s^{-1}sr^{-1}]	1.57×10^{-4}	1.43×10^{-4}	$+7.6\times10^{-6}$ -7.4×10^{-6}
K_{1-n} [PeV^{-1}m^{-2}s^{-1}sr^{-1}]	1.14×10^{-4}	1.05×10^{-4}	$+5.2\times10^{-6}$ -5.3×10^{-6}
K_{1-f} [PeV^{-1}m^{-2}s^{-1}sr^{-1}]	1.34×10^{-4}	1.23×10^{-4}	$+4.9\times10^{-6}$ -5.0×10^{-6}
γ_{11}	2.765	2.773	$+6.9\times10^{-3}$ -6.5×10^{-3}
$\Delta\gamma_{21-p}$	0.342	0.399	$+5.6\times10^{-2}$ -4.8×10^{-2}
$\Delta\gamma_{21-h}$	0.583	0.671	$+6.8\times10^{-2}$ -6.1×10^{-2}
$\Delta\gamma_{21-n}$	0.519	0.606	$+7.0\times10^{-2}$ -6.1×10^{-2}
$\Delta\gamma_{21-f}$	0.408	0.484	$+6.8\times10^{-2}$ -5.9×10^{-2}
$\Delta\gamma_{32}$	1.078	1.238	$+9.9\times10^{-2}$ -9.0×10^{-2}
E_{a-p} [PeV]	1.07×10^{-3}	1.27×10^{-3}	$+2.0\times10^{-4}$ -1.6×10^{-4}
E_{k1-p} [PeV]	2.45×10^{-2}	2.50×10^{-2}	$+7.0\times10^{-4}$ -1.4×10^{-3}
w_a	1.59	1.42	+0.14 -0.12
w_{k1}	1.00	1.00	$+5.2\times10^{-2}$ -2.4×10^{-2}
K_{2-p} [PeV^{-1}m^{-2}s^{-1}sr^{-1}]	1.70×10^{-4}	1.98×10^{-4}	$+8.0\times10^{-6}$ -8.5×10^{-6}
K_{2-h} [PeV^{-1}m^{-2}s^{-1}sr^{-1}]	7.93×10^{-5}	1.02×10^{-4}	$+8.1\times10^{-6}$ -8.9×10^{-6}
K_{2-n} [PeV^{-1}m^{-2}s^{-1}sr^{-1}]	4.50×10^{-5}	5.40×10^{-5}	$+9.0\times10^{-6}$ -8.2×10^{-6}
K_{2-f} [PeV^{-1}m^{-2}s^{-1}sr^{-1}]	2.63×10^{-5}	3.58×10^{-5}	$+3.9\times10^{-6}$ -4.0×10^{-6}
γ_2	2.37	2.42	+0.15 -0.16
$\Delta\gamma_2$	1.37	1.15	+0.09 -0.08
E_{k2-p} [PeV]	3.13	2.88	+0.17 -0.17
w_{k2}	2.99	3.69	+0.55 -0.41
K_{3-p} [PeV^{-1}m^{-2}s^{-1}sr^{-1}]	1.92×10^{-5}	1.00×10^{-5}	$+3.9\times10^{-6}$ -2.7×10^{-6}
γ_{3-p}	2.62	2.57	$+4.4\times10^{-2}$ -4.5×10^{-2}

Local source in the GeV-TeV energy range is not strictly necessary (!)

The rigidity of the GeV-TeV "ankle", of the TeV and PeV "knees" is the same for all spectra (!!)

The low-energy power-law index is the same for all spectra (!)

The "strength of the break" for the GeV-TeV ankle is probably different at least for protons and nuclei → the "propagation scenario" for the GeV-TeV ankle is disfavoured



Local source
is not strictly necessary →
cf. γ-ray datasets (Valenciano et al., astro-ph/2608.28757 (2026))

The GeV-TeV ankle corresponds to an ankle in the Galactic diffuse γ-ray spectrum; the energy of the ankle in the γ-ray spectrum is weakly dependent on the Galactic latitude
(if at all)

+secondary nuclei: see Subsect. 6.5 in astro-ph/2606.02748v2

Best-fit parameter values for proton, Helium, CNO, and Iron spectra

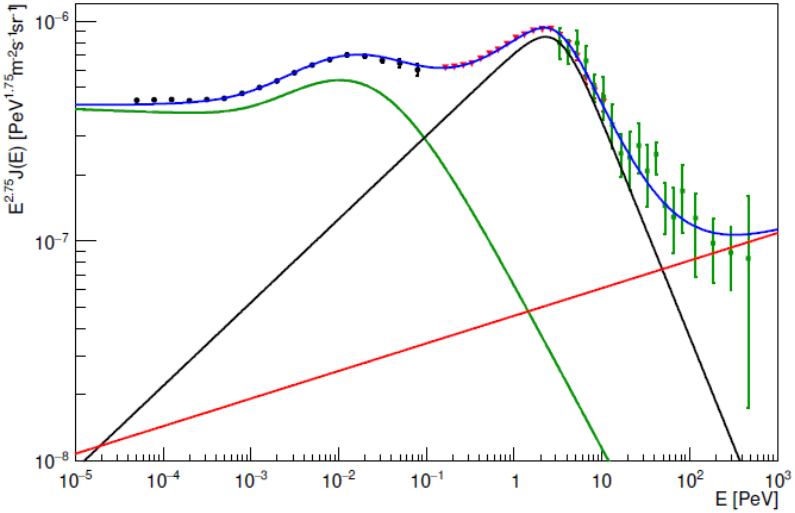
parameter	value (MIGRAD)	value (MCMC)	uncertainties (MCMC)
K_{1-p} [PeV^{-1}m^{-2}s^{-1}sr^{-1}]	1.96×10^{-4}	1.81×10^{-4}	$+9.6\times10^{-6}$ -9.4×10^{-6}
K_{1-h} [PeV^{-1}m^{-2}s^{-1}sr^{-1}]	1.57×10^{-4}	1.43×10^{-4}	$+7.6\times10^{-6}$ -7.4×10^{-6}
K_{1-n} [PeV^{-1}m^{-2}s^{-1}sr^{-1}]	1.14×10^{-4}	1.05×10^{-4}	$+5.2\times10^{-6}$ -5.3×10^{-6}
K_{1-f} [PeV^{-1}m^{-2}s^{-1}sr^{-1}]	1.34×10^{-4}	1.23×10^{-4}	$+4.9\times10^{-6}$ -5.0×10^{-6}
γ_{11}	2.765	2.773	$+6.9\times10^{-3}$ -6.5×10^{-3}
$\Delta\gamma_{21-p}$	0.342	0.399	$+5.6\times10^{-2}$ -4.8×10^{-2}
$\Delta\gamma_{21-h}$	0.583	0.671	$+6.8\times10^{-2}$ -6.1×10^{-2}
$\Delta\gamma_{21-n}$	0.519	0.606	$+7.0\times10^{-2}$ -6.1×10^{-2}
$\Delta\gamma_{21-f}$	0.408	0.484	$+6.8\times10^{-2}$ -5.9×10^{-2}
$\Delta\gamma_{32}$	1.078	1.238	$+9.9\times10^{-2}$ -9.0×10^{-2}
E_{a-p} [PeV]	1.07×10^{-3}	1.27×10^{-3}	$+2.0\times10^{-4}$ -1.6×10^{-4}
E_{k1-p} [PeV]	2.45×10^{-2}	2.50×10^{-2}	$+7.0\times10^{-4}$ -1.4×10^{-3}
w_a	1.59	1.42	+0.14 -0.12
w_{k1}	1.00	1.00	$+5.2\times10^{-2}$ -2.4×10^{-2}
K_{2-p} [PeV^{-1}m^{-2}s^{-1}sr^{-1}]	1.70×10^{-4}	1.98×10^{-4}	$+8.0\times10^{-6}$ -8.5×10^{-6}
K_{2-h} [PeV^{-1}m^{-2}s^{-1}sr^{-1}]	7.93×10^{-5}	1.02×10^{-4}	$+8.1\times10^{-6}$ -8.9×10^{-6}
K_{2-n} [PeV^{-1}m^{-2}s^{-1}sr^{-1}]	4.50×10^{-5}	5.40×10^{-5}	$+9.0\times10^{-6}$ -8.2×10^{-6}
K_{2-f} [PeV^{-1}m^{-2}s^{-1}sr^{-1}]	2.63×10^{-5}	3.58×10^{-5}	$+3.9\times10^{-6}$ -4.0×10^{-6}
γ_2	2.37	2.42	+0.15 -0.16
$\Delta\gamma_2$	1.37	1.15	+0.09 -0.08
E_{k2-p} [PeV]	3.13	2.88	+0.17 -0.17
w_{k2}	2.99	3.69	+0.55 -0.41
K_{3-p} [PeV^{-1}m^{-2}s^{-1}sr^{-1}]	1.92×10^{-5}	1.00×10^{-5}	$+3.9\times10^{-6}$ -2.7×10^{-6}
γ_{3-p}	2.62	2.57	$+4.4\times10^{-2}$ -4.5×10^{-2}

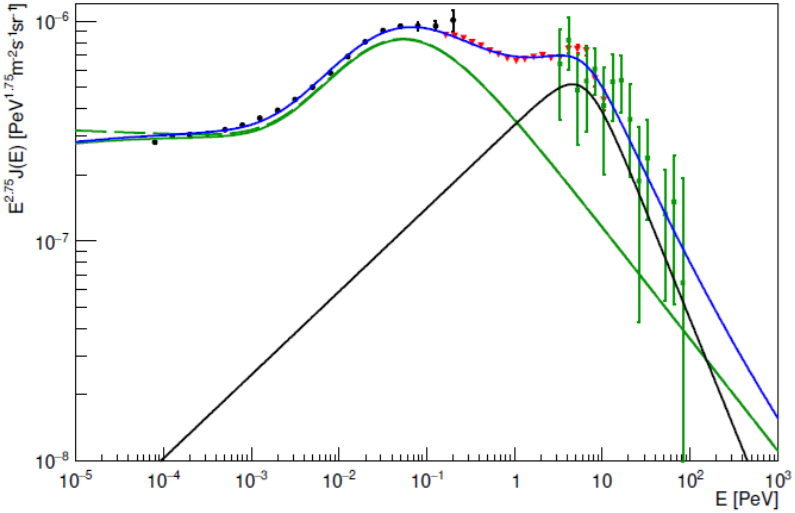
The rigidity of the GeV-TeV "ankle", of the TeV and PeV "knees" is the same for all spectra (!!)

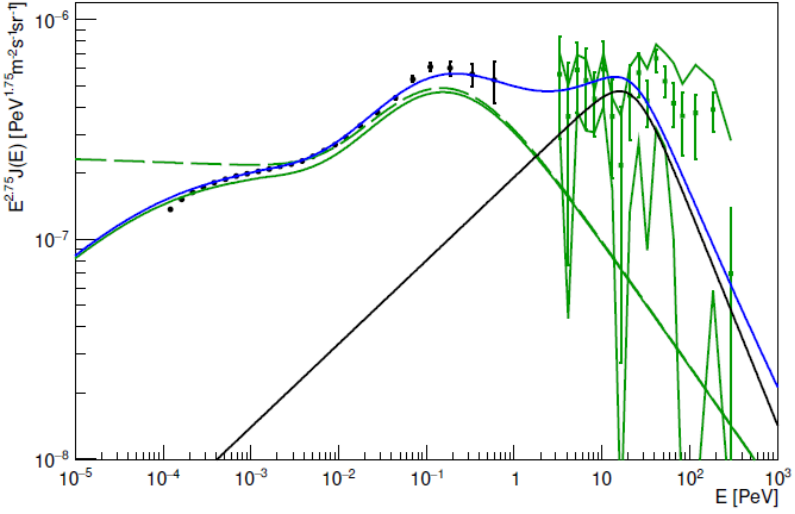
The low-energy power-law index is the same for all spectra (!)

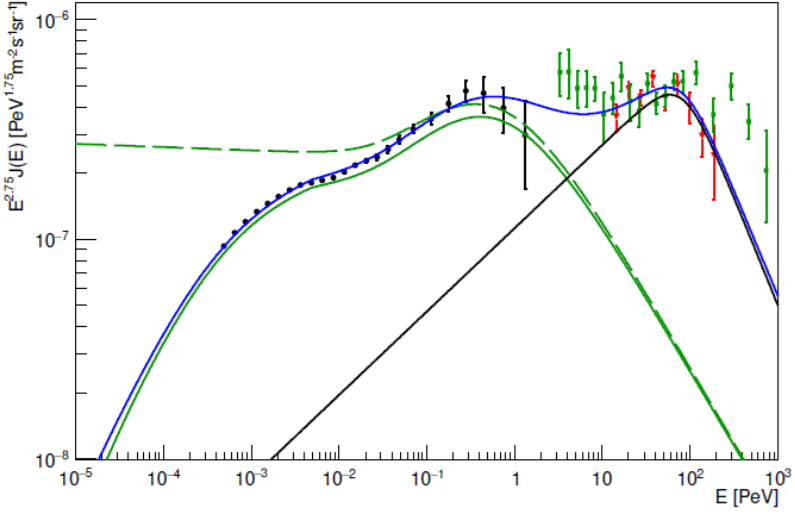
The "strength of the break" for the GeV-TeV ankle is probably different at least for protons and nuclei → the "propagation scenario" for the GeV-TeV ankle is disfavoured

Proton (top-left), Helium (top-right), CNO (bottom-left), and Iron spectra









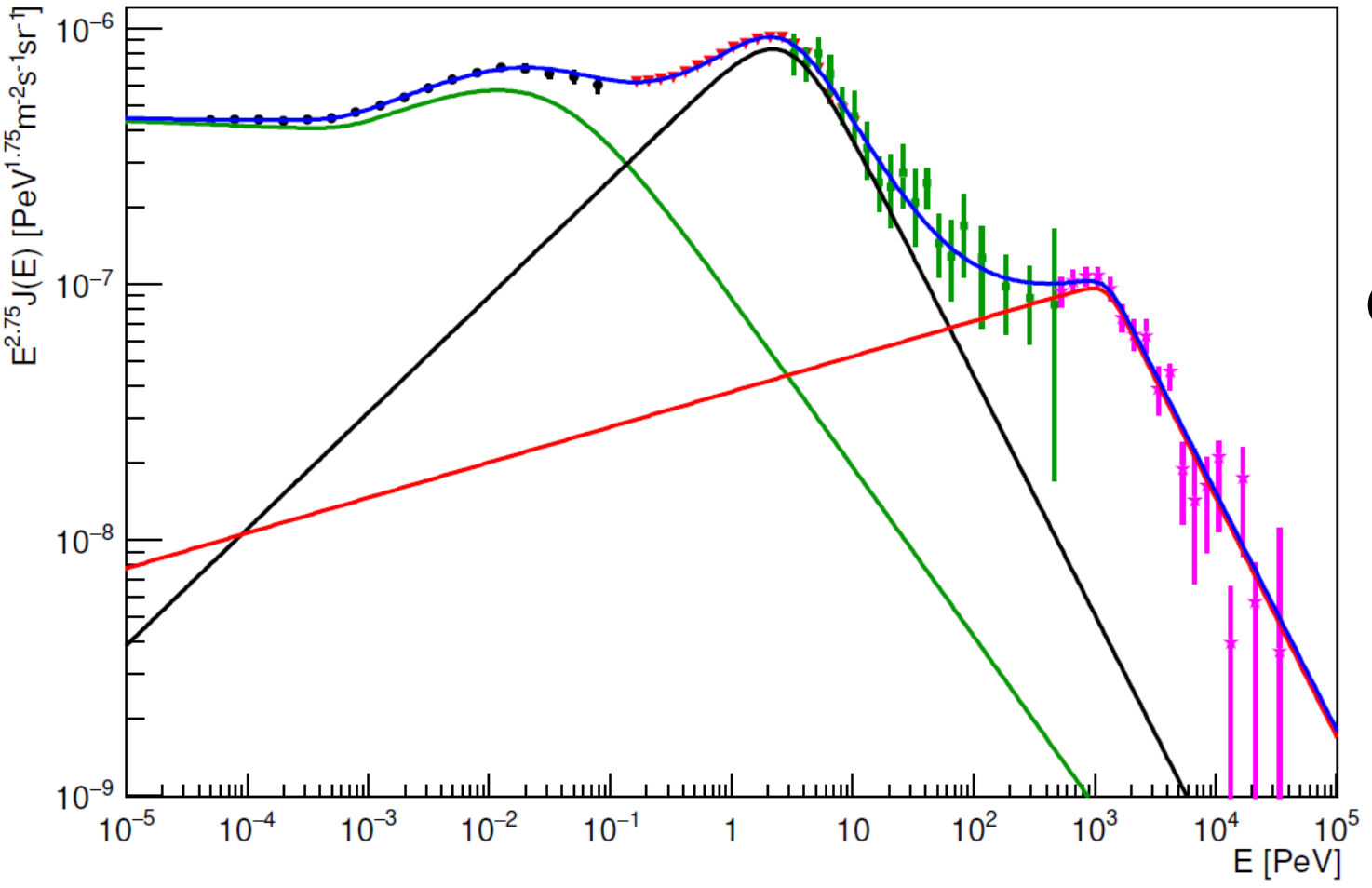
The datasets:

Helium: A26, LHAASO (Cao et al., 2026), Ice-Top (A19)

CNO: A26, Ice-Top (A19)

The effect of spallation is significant for the CNO and modest for the Helium spectrum

The proton CR spectrum: DAMPE (black circles), LHAASO ($K_E = 0.93$), EAS-Top ($K_E = 0.93$) +Auger measurements (Abdul Halim et al., 2026, $K_E = 0.95$)



The third component is well fitted with the SBPL functional form

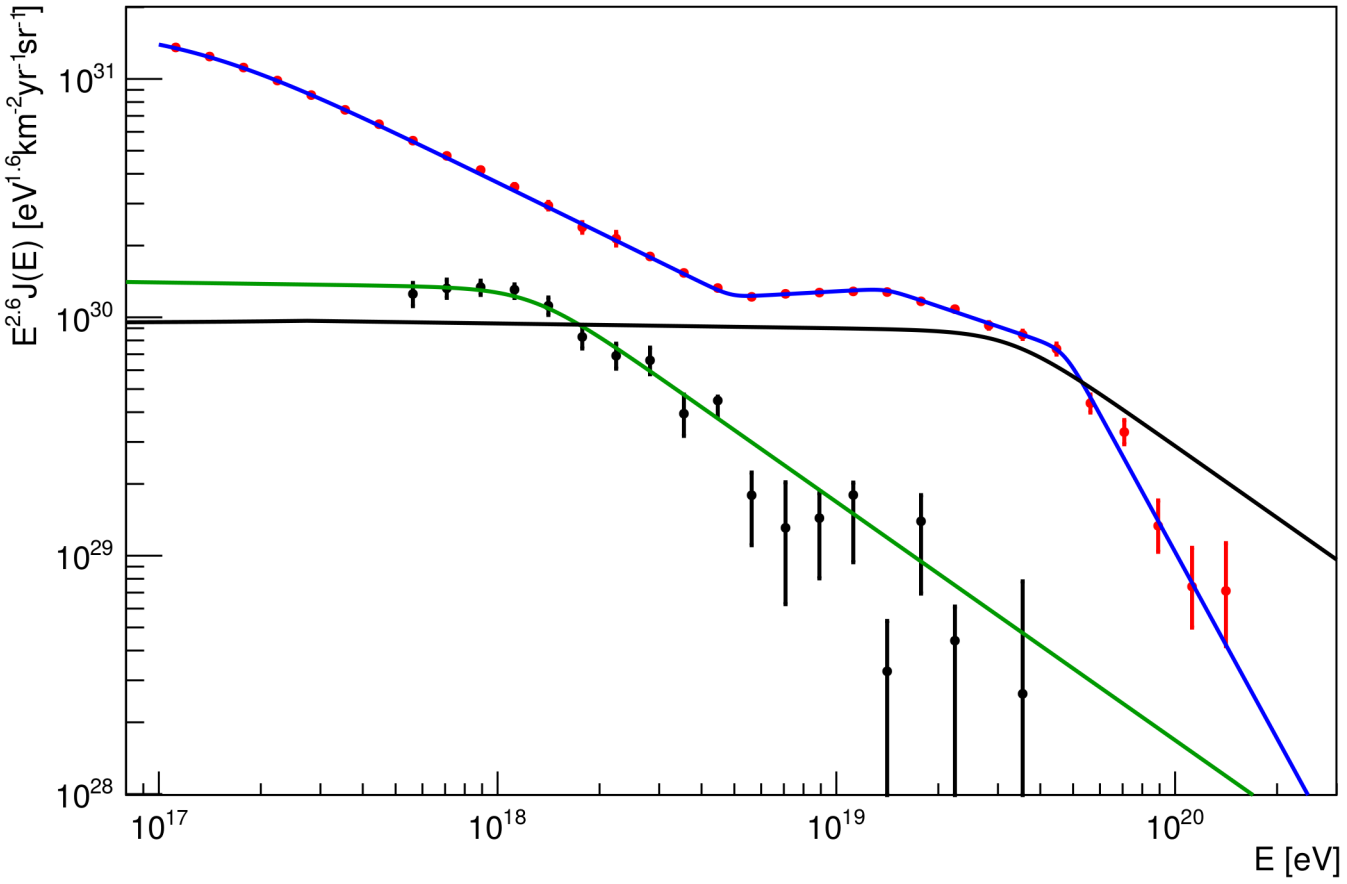
$\gamma_{31} = 2.61$, $\gamma_{32} = 3.68$,

$E_{k3} = 1.25$ EeV, $w_{k3} = 7.59$

(68 % C.L from 5.48 to 9.25)

Three populations of SNRs? The third component is due to hypernovae (Wang et al. (2007)) or engine-driven supernovae (Chakraborti et al. (2011))? Some contribution from GRBs?

The all-nuclei CR spectrum (Auger, Abreu et al. (2021)), the proton component (black circles, Abdul Halim et al. (2026)), the Iron component (a qualitative representation, before photodisintegration)



Comment on very low energies (1-40 GeV): need to add heliospheric modulation

With these additions, it may become possible to approximate the whole CR spectrum (1 GeV --- 100 EeV) with only three populations of SNRs

Conclusions

I. The proton CR spectrum consists of two Galactic components + one extragalactic component; all could come from distinct SNR populations.

II. The rigidity of the GeV-TeV ankle (E_a) and of all the knees (E_{k1}, E_{k2}, E_{k3}) could be the same for all elemental spectra (when leaving the source); the low-energy power-law index could be the same for all elemental spectra.

III. There is some indication that $\Delta\gamma$ in GeV-TeV ankle for nuclei is greater than for protons → the propagation scenario for this feature is disfavoured.

IV. The local source in the GeV-TeV energy range is not strictly necessary (cf. γ-ray datasets).

This work was supported by the Russian Science Foundation, grant no. 22-12-00253-P.